Journal of Physics:
Conference Series

PAPER • **OPEN ACCESS**

SOFC-based propulsion systems for maritime applications

To cite this article: G. Di Cicco *et al* 2025 *J. Phys.: Conf. Ser.* **3143** 012095

Journal of Physics: Conference Series **3143** (2025) 012095 doi:10.1088/1742-6596/3143/1/012095

SOFC-based propulsion systems for maritime applications

G. Di Cicco[1*], B. Rinauro[1], A. Perna[1], D. Lanni[1] and M. Minutillo[2]

[1] Department of Civil and Mechanical Engineering, University of Cassino and Southern Lazio, Cassino, Italy
[2] Department of Industrial Engineering, University of Salerno, Fisciano, Italy

*E-mail: gabriella.dicicco@unicas.it

Abstract. The decarbonization of maritime transport is a crucial issue in recent times, since this sector continues to account for approximately 2.8% of the global CO_2 emissions. To address this issue, various proposals have been put forward to promote the utilization of renewable and low/zero carbon fuels in marine applications. In this context, this study aims to define different configurations of innovative naval propulsion systems utilizing Solid Oxide Fuel Cells (SOFC) fed by ammonia. A particular case study has been examined, focusing on a vessel with a known mission profile and engine room hosting a conventional internal combustion engine. The analysis explores the possibility of incorporating the proposed SOFC-based propulsion system into this vessel by considering the weights and volumes of the modules and onboard fuel storage. Each SOFC module includes not only the stacks but also their Balance of Plant (BoP) components, such as the afterburner and multiple heat exchangers designed to enhance heat recovery and maximize system efficiency. In particular, the proposed configuration is assessed in terms of fuel consumption and design compactness, taking into account specific constraints such as its mission profile and the available space in the engine room of the considered vessel. The analysis is carried out through properly developed thermochemical models able to determine the operational characteristics of the system, while also taking into account the thermal management of the modules.

1. Introduction

The maritime sector accounts for over 2% of global CO_2 emissions associated with the energy system [1]. Traditionally, marine propulsion has relied on fossil-based fuels such as Marine Gas Oil (MGO) and Heavy Fuel Oil (HFO), which not only contribute to greenhouse gas emissions but also release harmful pollutants like nitrogen oxides and sulphur compounds [2]. While mitigation strategies such as biofuel adoption and energy efficiency improvements are being explored, achieving full decarbonization requires a radical shift toward alternative fuels and innovative propulsion technologies.

This transition from conventional marine powertrains to cleaner alternatives involves replacing internal combustion engines (ICEs) with fuel cells, electrochemical devices that convert the chemical energy of fuels (mainly hydrogen or hydrogen-rich compounds such as ammonia) into electrical energy in the form of direct current. This generated electricity can thus be utilized to power electric motors for ship propulsion.

Researchers in the maritime sector are increasingly focusing on Solid Oxide Fuel Cells (SOFC), which, despite limited current use, are seen as the best long-term propulsion solution due to their high power output and efficient operation with various fuels, including ammonia [3]. As a matter of fact, ammonia is being progressively accepted as a suitable carbon-free energy carrier for marine applications due to its high hydrogen content, well-established transport and storage infrastructure [4]–[6]. Compared to hydrogen, it offers higher volumetric energy density and is easier to store under ambient or moderately pressurized conditions. However, ammonia's toxicity and the need for onboard cracking or fuel processing remain key technical challenges.

Recent studies have shown a growing interest in the use of ammonia-powered SOFC-based systems for maritime propulsion. Di Micco et al. [7] analysed the technical feasibility of replacing traditional diesel engines in commercial ships with ammonia-fuelled SOFC systems. Their research assessed the system's ammonia consumption and found that the size of the SOFC powertrain that met the energy requirements exceeded the available engine room volume by 9%. Koekkoek [8] introduced and modelled a hybrid propulsion system that integrates ammonia-fuelled solid oxide SOFCs with internal combustion engines for use in naval applications. The findings suggested that the hybrid system has the potential to exceed the efficiency of conventional internal combustion engines, although the author identified potential challenges related to system size and NO_x emissions. Kalstad [9] performed experimental studies on a solid oxide fuel cell destined for marine applications and powered by aqueous ammonia solutions of different concentrations. The research indicated that greater ammonia concentrations ensured high power densities, with the 32% solution demonstrating performance similar to pure hydrogen feeding at higher temperatures.

While numerous studies have investigated ammonia-fuelled SOFC systems, the majority have concentrated on hybrid setups or general feasibility assessments, whereas there is a lack of comprehensive thermochemical modelling of standalone SOFC powertrains directly fed with ammonia for maritime applications. This paper proposes to address this gap by evaluating the feasibility and integration of an ammonia-powered SOFC propulsion system for a passenger vessel.

2. Materials and Methods

The approach followed in this research (Figure 1) starts from the identification of a reference vessel and the evaluation of its main characteristics, including power demand, typical voyage patterns, and engine room layout. Based on this analysis, an innovative SOFC-based power system is designed and modelled to meet the vessel's energy requirements, and its fuel consumption is subsequently estimated and compared with the conventional configuration. The proposed system's performances are evaluated against that of the conventional ICE in terms of fuel consumption, system efficiency, and reduction in pollutant and climate-altering emissions. Finally, the proposed SOFC-based propulsion system is evaluated in terms of its integration within the vessel's existing engine room, taking into account volume and weight constraints.

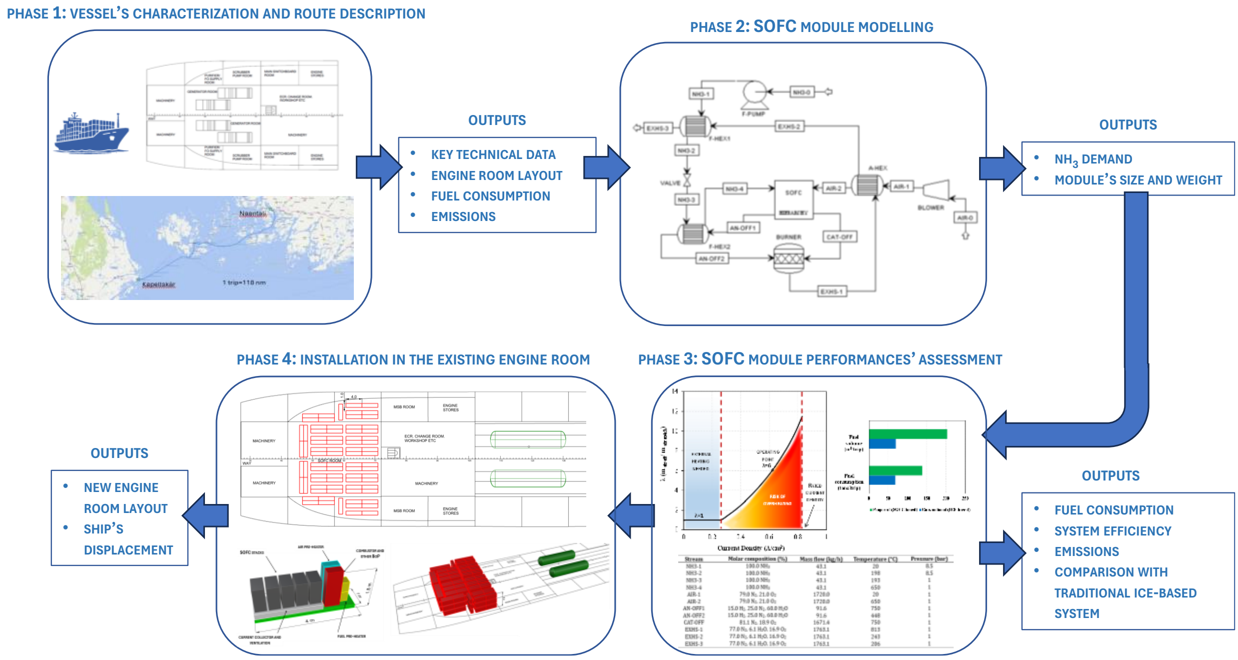

Figure 1. Methodology workflow

2.1 Vessel characterization and route description

To begin with, a ship was selected as the reference vessel. The chosen vessel to integrate the new SOFC-based technology is a passenger ferry operating in Northern Europe, navigating through the Archipelago Sea. In particular, the ship considered in this study is based on a design project presented in [10], which focuses on enhancing the manoeuvrability of an existing vessel in shallow waters — a key performance factor given the short and repetitive route on which the ferry operates. The ship's main characteristics are presented in Table 1.

Table 1. Ship main characteristics

Parameter	Unit	Value
Length overall	m	230
Length between perpendiculars	m	216
Moulded breadth	m	33.6
Scantling draft	m	7.1
Displacement	m	34540
Speed Design	kn	16
Max Speed	kn	20

The ship operates daily on a round-trip route between Naantali and Kapellskär with a stop in Lumparland, as shown in Figure 2, covering approximately 236 nautical miles. Each trip involves around 8 hours at sea and about 3.8 hours in port.

Since the ship spends a significant amount of time navigating narrow waters with frequent route changes, the original propulsion system, based on two shaft lines, has been replaced with an azipod propulsion system. This upgrade enhances manoeuvrability, especially at low speeds and during mooring operations. In the updated propulsion configuration, the vessel's azipod units and onboard electrical systems are powered by four Wärtsilä 12V32 generator sets, each rated at 6960 kW, for a total installed power of 27,840 kW. At the vessel's maximum speed of 20 knots with all four engines operating, the generators run at 85% of their Maximum Continuous Rating (MCR). At the design speed of 16 knots with three engines in operation, the load drops to approximately 64% MCR.

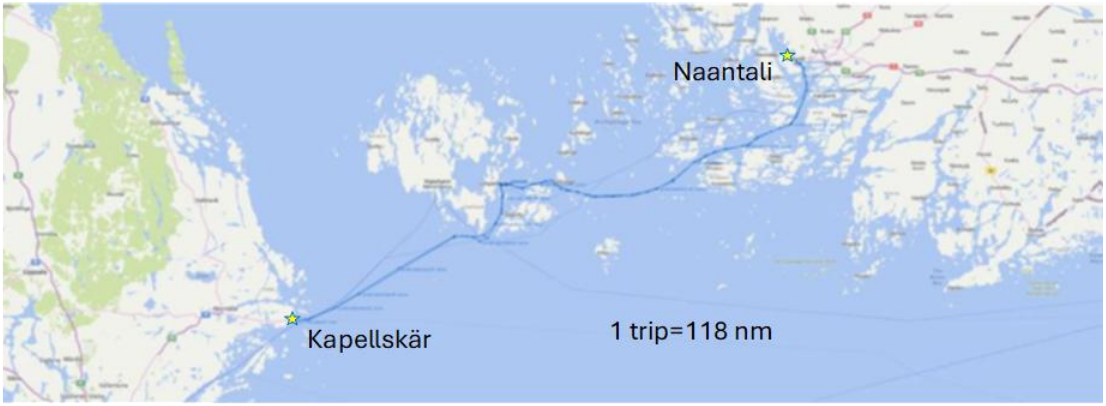

Figure 2. Itinerary between Naantali – Kapellskär

For the purposes of this preliminary study, it reasonabile to assume a constant load for estimating fuel consumption and emissions over a round trip. Therefore, the vessel's fuel consumption per round trip $m_{fuel_{trip}}$ is calculated as:

$$m_{fuel_{trip}} = SFC \cdot f_{MCR} \cdot n_{active_{engines}} \cdot h_{trip} \quad (1)$$

where SFC is the specfic fuel consumption corresponding to the engine load, expressed as a fraction f_{MCR} of the MCR, while $n_{active_{engines}}$ is the number of running engines and h_{trip} is total trip duration (Naantali – Kapellskär and back) expressed in hours. To ensure a conservative estimate of the fuel consumption, the vessel is assumed to cruise continuously at 20 kn. According to the engine datasheet, under these conditions, the SFC is 180 g/kWh [11], resulting in a daily fuel consumption of 68.5 tons on the Naantali–Kapellskär route. Considering the ferry's brief and highly repetitive route, likely characterized by minimal variation in power demand during cruising, it is reasonable, for the purposes of this preliminary study, to assume a constant load for estimating fuel consumption and emissions over a round trip.

Finally, based on the total fuel consumption per voyage, the main emissions (CO_2, NO_x, SO_x, and PM) have been estimated through their respective emission factors, as reported in Table 2.

Table 2. Emissions per voyage

Compound	Emission Factor (kg/kg)	Emission per trip (ton)
CO_2	3.114	213.3
NO_x	0.077	5.3
SO_x	0.047	3.21
PM	0.007	0.5

The engine room configuration with four diesel engines is illustrated in Figure 3. A single diesel engine measures approximately 10.7 meters in length, 3 meters in width, and 4.1 meters in height, resulting in a volume of about 135 m^3. Its estimated weight is around 100 metric tons.

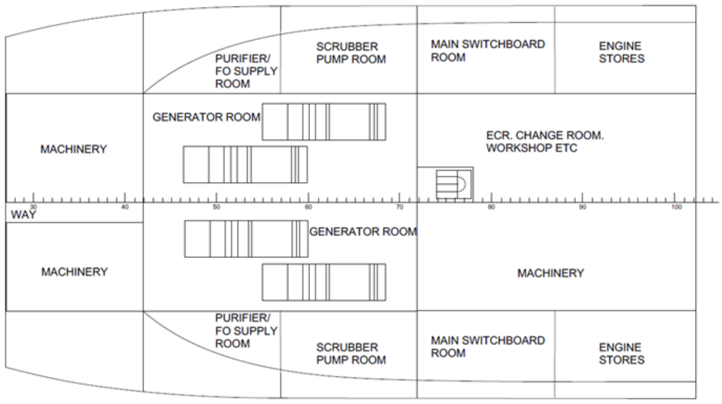

Figure 3. Engine room configuration

2.2 SOFC module modelling

The next phase of the study focuses on developing a thermochemical and electrochemical model of a solid oxide fuel cell directly fed with ammonia. The proposed power generation system, which is based on SOFC technology, has been designed with a modular architecture, in which the SOFC module serves as the core system. The initial step in the design of the module involves selecting the SOFC stack. For this purpose, the architecture of a 30 kW SOFC stack manufactured by Solydera, has been taken as a reference [12]. This stack consists of 400 cells, each with an active area of approximately 200 cm^2. To evaluate the operating conditions and performance of this stack when using ammonia, a numerical model has been developed. Details regarding the model and its validation can be found in the Appendix. Table 3 provides a summary of the operating data of the stack when directly fed with ammonia. It is important to highlight that the stack's net rated power (calculated by subtracting the Balance of Plant power, absorbed by the auxiliary components of the entire module) is 30 kW, and its efficiency, based on the lower heating value (LHV) of ammonia, is 52.4%.

Table 3. Operating data and performance of the SOFC stack fed by ammonia

Operating Parameters	Unit	Value
Temperature	°C	750
Anode feed	mol %	NH_3, 100
Anode feed consumption at rated power	kg/h	10.9
Current at rated power	A	102.7
Voltage at rated power	V	321.9
Gross Power	kW	33.1
BoP consumption	% of Gross Power	9%
Rated power	kW	30.0
Stack efficiency at rated power	%	52.4%

The next phase in the module's design focuses on the definition of its layout. Each module consists of: i) four interconnected stacks that share a common Balance of Plant (BoP), a catalytic burner to recover thermal energy from both anodic and cathodic exhausts, and iv) heat exchangers necessary to pre-heat the feed streams entering the stacks. Furthermore, the module is insulated to reduce heat loss to the environment, and is equipped with all necessary auxiliary components for electric conditioning (including, DC/AC inverters, transformers, switchboards, and control units) as well as pumps and blowers.

To identify the optimal operating conditions and evaluate the performance of the module, a numerical model has been developed through the Aspen Plus software. This model, whose flowsheet is shown in Figure 4, is made up of operational blocks designed to simulate the SOFC unit, heat exchangers, and reactors, interconnected through mass and energy flows.

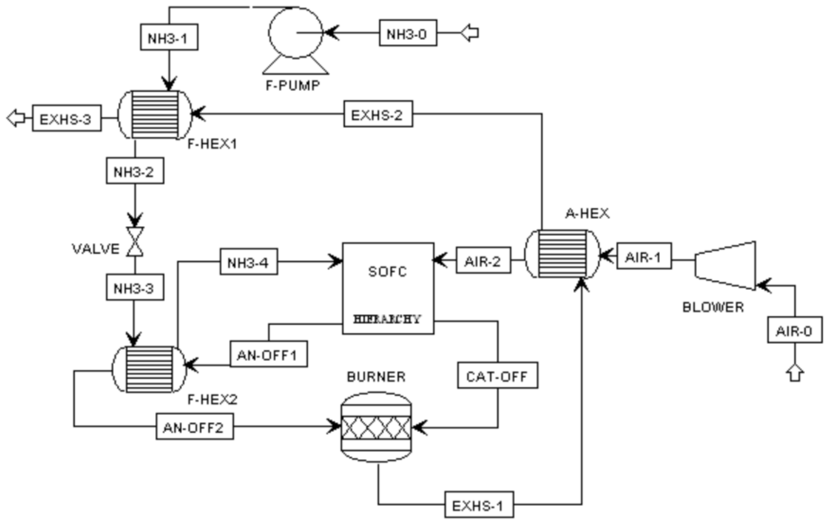

Figure 4. Flowsheet of the 120 kW SOFC module model

The achievement of the module's thermal self-sustainment is ensured through the optimization of heat recovery from the hot streams, specifically the anode off-gas (AN-OFF). In fact, these streams serve as hot fluids in heat exchangers A-HEX and F-HEX 1, and F-HEX2, respectively, to preheat both the air (AIR) and ammonia (NH3). In fact, ammonia, initially stored as a pressurized liquid at 20 °C and 8.5 bar, is heated together with the air to the required inlet temperature before entering the stacks to minimize thermal stresses (a temperature difference of 100 °C between the stacks and the reactant gases has been set). Furthermore, between the two pre-heating stages, ammonia is expanded through a valve to reach the operating pressure of the fuel cell stacks.

The module's net power output P_{Module}, destined to propulsion or onboard auxiliary utilities, is calculated as in eq. (2):

$$P_{Module} = N_{Stack}(P_{Stack} - P_{BoP}) \quad (2)$$

where P_{BoP} is the power consumed by the BoP auxiliary components.

The module's efficiency is:

$$\eta_{Module} = \frac{P_{Module}}{\dot{m}_{NH_3} \cdot LHV_{NH_3}} \quad (3)$$

3. Results and Discussion

This section presents the main results of the system-level model of the ammonia-fed SOFC module, focusing on its physical layout, operating strategy, and comparative performance against a conventional diesel-based configuration.

3.1 SOFC module performance's assessment

Considering that the designed module is made up of four stacks, the net rated power (obtained by subtracting the power consumed by the Balance of Plant from the gross power output of the module) under rated conditions is 120 kW. This size is technically feasible, as demonstrated by AlmaClean Power's recent successful testing of a 100 kW direct ammonia-fed SOFC module for marine applications [13].

The results of the model regarding the operating conditions of each stream at rated power, along with the mass balances, are summarized in Table 4.

Table 4. Module's mass balance and process streams' operating conditions

Stream	Molar composition (%)	Mass flow (kg/h)	Temperature (°C)	Pressure (bar)
NH3-1	100.0 NH_3	43.9	20	8.5
NH3-2	100.0 NH_3	43.9	257	8.5
NH3-3	100.0 NH_3	43.9	253	1
NH3-4	100.0 NH_3	43.9	650	1
AIR-1	79.0 N_2, 21.0 O_2	1027.1	20	1
AIR-2	79.0 N_2, 21.0 O_2	1027.1	650	1
AN-OFF1	15.0 H_2, 25.0 N_2, 60.0 H_2O	93.3	750	1
AN-OFF2	15.0 H_2, 25.0 N_2, 60.0 H_2O	93.3	484	1
CAT-OFF	81.1 N_2, 18.9 O_2	977.7	750	1
EXHS-1	77.0 N_2, 6.1 H_2O, 16.9 O_2	1071.0	856	1
EXHS-2	77.0 N_2, 6.1 H_2O, 16.9 O_2	1071.1	302	1
EXHS-3	77.0 N_2, 6.1 H_2O, 16.9 O_2	1071.1	233	1

The nominal operating point of the module is 85% of the rated power, which corresponds to a net power output of 103.2 kW. At this load, the system operates with an average current density of 0.43 A/cm^2 and a cell voltage of 0.83 V, resulting in a net electrical efficiency of 53.4% and a specific fuel consumption of 429.5 g/kWh. These values, along with the trends of fuel consumption and efficiency for different load levels, are illustrated in Figure 5, which depicts the module's fuel consumption and efficiency's variation with varying loads.

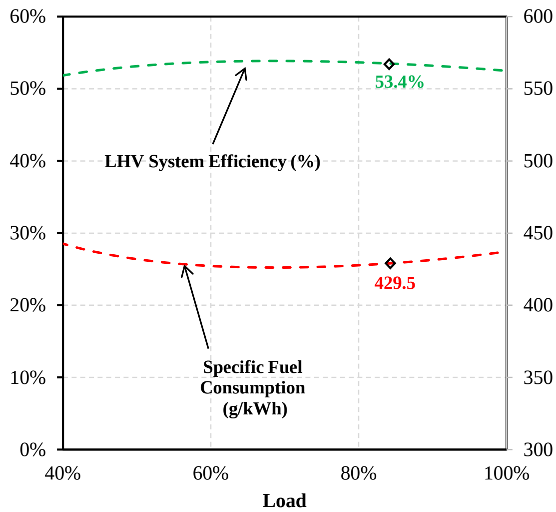

Figure 5. Module's specific fuel consumption (red) and efficiency (green) vs. load

In addition, a suitable thermal management strategy was defined to ensure stable operating conditions of the modules. This strategy involves varying the air mass flow on the cathode side with the module's load in order to minimize net heat generation within the cells, thus avoiding the need for dedicated cooling systems. This approach also helps maintain the temperature of the anode and cathode streams at 650 °C, thus avoiding linear thermal gradients greater than 10 °C/cm, and reducing the risk of thermal stresses that could compromise the mechanical integrity of the cells [14], [15]. These conditions cannot be fully achieved at very low loads (below 20%) where the cells' voltage losses are minimal and therefore insufficient heat is generated internally to sustain the desired operating temperature thus, external heating would be needed. However, these low-load conditions are typically reached only during transients or start-ups, therefore this effect can be overlooked in the present preliminary study. At nominal operating conditions (85% of the load), the excess air coefficient λ is equal to 5.71, increasing to 7.73 at rated power. This trend is illustrated in Figure 6, which shows the variation of λ with module's load.

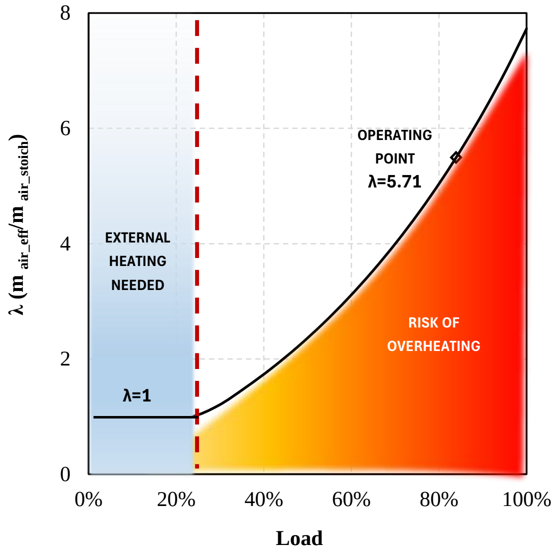

Figure 6. Excess air coefficient (λ) vs. load for the SOFC module. In blue, current density values where additional heating is needed; in red, λ values which could cause overheating.

To assess the feasibility of physically replacing the marine engine, a 125 kW SOFC module originally designed to operate on methane was taken as a reference for its size and weight's estimate [16]. This approach is conservative, given that the ammonia-fed module has a comparable rated power output but a simplified architecture, as it does not require the reformer and steam boiler included in the methane-based design. Figure 7 shows a schematic depiction of the modelled 120 kW SOFC module, while Table 5 reports its estimated dimensions and weight.

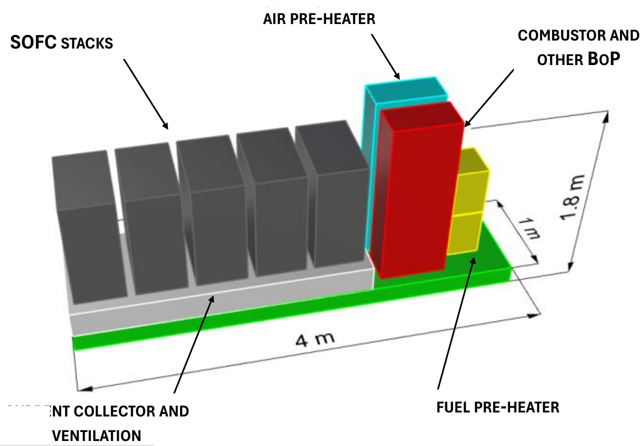

Figure 7. Schematic depiction of a direct ammonia 120 kW SOFC-based module

Table 5. 120 kW direct ammonia SOFC module's weight and dimensions.

Parameter	Unit	Value
Length	m	4
Width	m	1
Height	m	1.8
Weight	ton	6.8

To determine the potential benefits of replacing conventional marine engines, the performance of the ammonia-fed SOFC module was compared with the vessel's existing diesel-based propulsion system. To match the maximum power provided by the traditional ICEs installed onboard of the vessel, the ammonia-based system requires 232 SOFC modules, each delivering a net output of 120 kW. At average operating conditions (85% of the rated power), each module requires 36.9 kg/h of liquid ammonia, resulting in a total ammonia consumption of 138.2 tons for a round trip. This higher consumption is a result of ammonia's lower heating value (18.8 MJ/kg) compared to that of HFO (~40.5 MJ/kg). The corresponding fuel volume required per voyage is approximately 202.5 m^3/day, calculated using a liquid ammonia density of 682 kg/m^3 [17], which is more than double that of HFO (69.2 m^3) due to ammonia's lower density. Furthermore, the propulsion system based on SOFC technology is significantly heavier than the conventional system: in fact, the overall weight of this innovative propulsion system is 1577 tons, which is almost 4 times greater than the combined weight of the four internal combustion engines used in the traditional setup. Figure 8 provides a summary of these results.

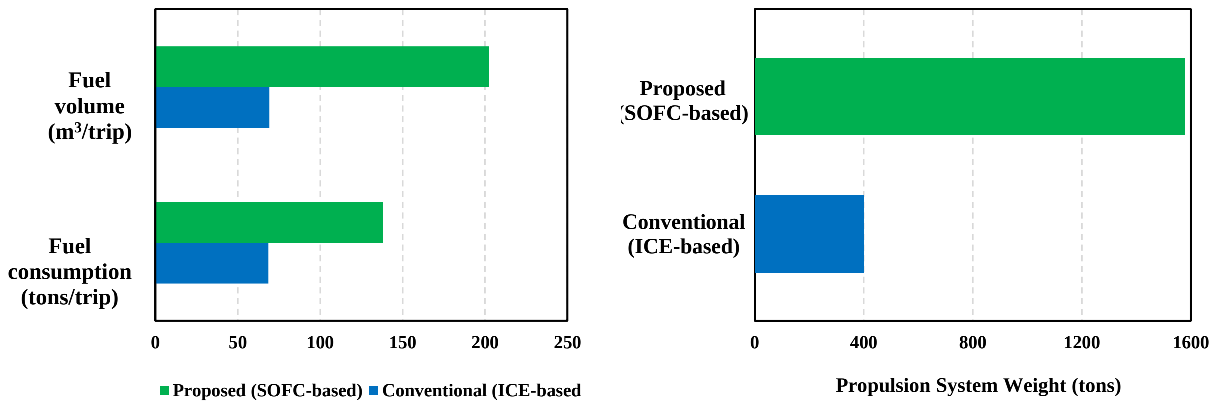

A) B)

Figure 8. Conventional and SOFC-based propulsion system's fuel volume and consumption (A) and weight (B)

Despite the increased fuel mass and volume, the ammonia-fed SOFC system provides considerable environmental benefits. As a matter of fact, since ammonia's molecules are carbon-free, CO_2 emissions are completely avoided. Additionally, due to the relatively low operating temperatures of the modules and the afterburner (750°C and 813 °C, respectively) the formation of thermal NO_x is minimal. Sulphur oxides (SO_x) and particulate matter (PM) emissions are also eliminated, as there are no sulphur and carbon-based compounds in the fuel.

3.2 SOFC modules' installation in the existing engine room

Regarding the layout of the modules within the engine room, a total of 232 units have been installed in the diesel engine rooms and the purifier and supply room, as illustrated in Figure 8. The modules are arranged in blocks of four units, with each block having two free sides and an 80 cm clearance surrounding it, to ensure accessibility for maintenance or replacing operations. These blocks are distributed across three vertical levels, with approximately 50 cm spacing between each level, resulting in a total structure height of about 6.4 meters. This configuration fits within the engine room, which has an overall height of approximately 7.5 meters.

Two pressurized ammonia tanks, operating at 8.5 bar and 20 °C, each with a storage capacity of approximately 220 m^3, have been included to ensure sufficient autonomy for two daily trips. The tanks are installed on the first garage deck, occupying an area equivalent to 150 lane meters. The total footprint is approximately 450 m^2, with dimensions of around 25 meters in length and 18 meters in width. Assuming each lane meter accounts for approximately 2.5 tonnes, 150 lane meters would correspond to a total weight of about 380 tonnes. Given that the weight of ammonia per tank is around 150 tonnes, the estimated weight of two tanks makes the total roughly comparable to the weight of the cargo lane.

Regarding the increased weight in the engine room, the difference between the weight of the diesel engines (approximately 400 tonnes) and the 232 SOFC units (about 1577 tonnes) is around 1200 tonnes. This corresponds to roughly 3% of the ship's total displacement and can be considered negligible at this preliminary stage of the analysis.

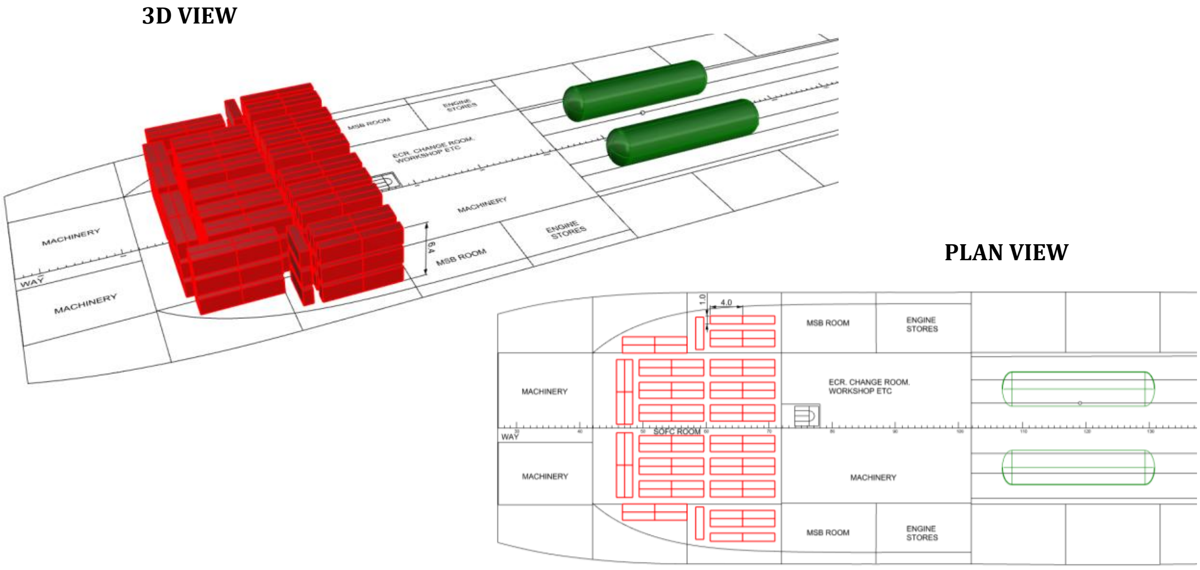

Figure 9. Engine room layout with SOFC modules and ammonia tanks

Regarding safety considerations, the primary concern associated with ammonia lies in its toxicity and gas dispersion characteristics. Currently, the only established rules and guidelines pertain to ammonia tankers: the IGC Code, which covers the transport of ammonia as cargo, and the IBC Code, which applies to aqueous ammonia.

In light of this, the general design requirements for the engine room include: proper ventilation systems, dedicated ammonia venting to the atmosphere, ammonia leak detectors to mitigate toxicity risks, implementation of a double-wall containment concept, mechanical protection for ammonia-containing components to prevent damage, and strict operational safety procedures.

4. Conclusions

This study investigates the feasibility of replacing a conventional marine propulsion system—comprising four Wärtsilä 12V32 engines with a total installed power of 27.8 MW—with a SOFC-based system directly fed with ammonia. The proposed configuration uses 232 SOFC modules, each delivering a rated power of 120 kW, to match the vessel's propulsion needs. At average operating conditions, the ammonia-fuelled SOFC system achieves a net electrical efficiency of 53.4%, while entirely avoiding CO_2, SO_x, and PM emissions, and significantly reducing NO_x formation. In order to provide the same amount of power as the conventional installed engines, the SOFC-based system requires 138.2 tons of ammonia daily—over twice the 68.5 tons of diesel utilized in the traditional configuration—resulting in a daily fuel volume of 202.5 m^3 compared to 69.2 m^3. While the proposed system is heavier and requires more storage capacity, it presents considerable environmental advantages. Furthermore, in spite of the increased system weight, the layout analysis confirmed that the modules and ammonia storage can be arranged within the existing vessel structure with minor modifications.

Appendix

The module's design is based on a validated single-cell model developed to simulate the behaviour of a SOFC directly fuelled with ammonia. The model, developed in Aspen Plus and shown in Figure A1, integrates both the chemical decomposition of ammonia and the electrochemical conversion of hydrogen and oxygen in water and electricity. The electrochemical modeling is carried out externally, through a Fortran-based user block, whereas mass and energy balances are addressed through conventional Aspen Plus blocks.

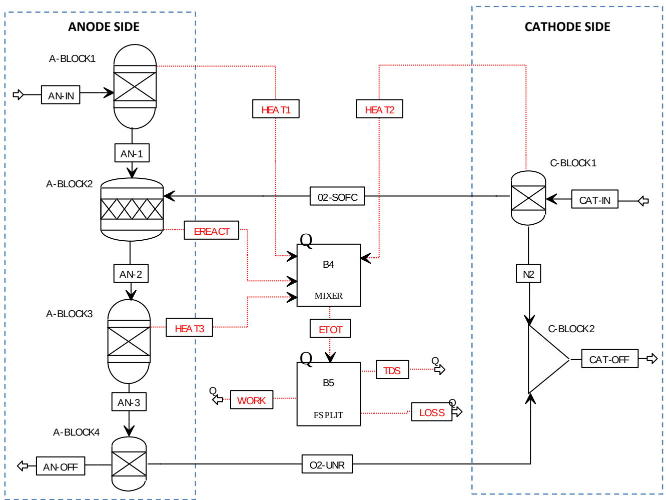

Figure A1. Flowsheet of the Aspen Plus cell model

The anodic compartment is represented by a Gibbs reactor (A-BLOCK1) that accounts for the decomposition of ammonia occurring on the Ni-based electrode, followed by a stoichiometric reactor (A-BLOCK2) which models the electrochemical oxidation of hydrogen. The oxidation of carbon monoxide is excluded from the model, as the electrochemical contribution of CO is typically negligible, with hydrogen responsible for over 98% of charge transfer reactions. On the cathode side, oxygen is separated from air using blocks C-BLOCK1 and A-BLOCK3 and sent to the anode, ensuring the correct stoichiometric ratio for the fuel reaction. The cell's thermal behaviour is modelled thanks to Q-MIXER and Q-SPLIT blocks, which deal with internal heat flows. The electrochemical sub-model consists of a set of semi-empirical equations (Eqs. A1–A14, Table A1) which detail the voltage losses attributed to activation, ohmic, and concentration overpotentials.

Table A1. SOFC model equations

Explanation	Equation
The model calculates the SOFC's effective voltage (1) by subtracting polarization losses from the reversible voltage E_{rev}, (2), assumed equal to the Nernst potential and estimated by interpolating standard Gibbs free energy values ΔG_0 (3) over the 500–1100 °C range [18]. Species partial pressures, p_k, are derived as the average between inlet and outlet compositions.	$V_{cell} = E_{rev} - \eta_{act,a/c} - \eta_{ohm} - \eta_{conc,a/c} - \eta_{leakage}$ (A1) $E_{rev} = E_0 + \frac{RT}{nF} ln\left(\frac{p_{H_2} \cdot p_{O_2}^{0.5}}{p_{H_2O}}\right)$ (A2) $E_0 = -\frac{\Delta G_0}{nF} E_0$ (A3)
Activation overpotentials (4) are modelled using the hyperbolic sine form of the Butler–Volmer equation [5], where α_i is the charge transfer coefficient, and n is the number of electrons exchanged. The exchange current density j_{0_i} (5) (6) is expressed through Arrhenius-type relations including pre-exponential factors γ_a and γ_c and activation energies $E_{act,a}$ and $Eact, c$ [19], [20]. Partial pressures at the triple-phase boundary $p_{i,TBP}$ are evaluated using Equations (7)-(9). Two transport mechanisms are considered to model the species' diffusivity according to the Dusti Gas Model : Knudsen diffusion $D_{i,K}$, based on kinetic gas theory [21], [22]; and molecular diffusion D_{A-B} calculated with Fuller's method [23], [24].	$\eta_{act,i} = \frac{RT_{cell}}{\alpha_i n_e F} \cdot sinh^{-1}\left(\frac{j}{2j_{0,i}}\right)$ (A4) $j_{0_a} = \gamma_a \left(\frac{p_{H_2TPB}}{p_{ref}}\right)\left(\frac{p_{H_2O_{TPB}}}{p_{ref}}\right) \cdot exp\left(-\frac{E_{act,a}}{RT}\right)$ (A5) $j_{0_C} = \gamma_C \left(\frac{p_{O_{2TPB}}}{p_{ref}}\right)^{0.25} \cdot exp\left(-\frac{E_{act,c}}{RT}\right)$ (A6) $p_{H_{2TPB}} = p_{H_2} - \frac{jRTt_a}{nFD_{eff_a}},$ (A7) $p_{H_2O_{TPB}} = p_{H_2O} + \frac{jRTt_a}{nFD_{eff_a}}$ (A8) $p_{O_{2TPB}} = p - (p - p_{O_2})\, exp\left(\frac{jRTt_c\delta_{O2}}{4FD_{eff_c}p}\right)$ (A9)
Ohmic losses (16) are calculated via Ohm's law. The total internal resistance R_{ohm} (17) is determined from the thickness t_i and conductivity of each cell component, with σ_i estimated via Arrhenius expressions [25].	$\eta_{ohm} = R_{ohm} \cdot j$ (A10) $R_{ohm} = \frac{\sigma_a}{t_a} + \frac{\sigma_c}{t_c} + \frac{\sigma_e}{t_e}$ (A11)
Concentration losses are introduced to account for species pressure gradients between the electrodes and the TPB region, following the approach in [21].	$\eta_{conc,a} = \frac{RT}{2F} \ln\left(\frac{p_{H_2O_{TPB}} \cdot p_{H_2}}{p_{H_2O} \cdot p_{H_{2TPB}}}\right)$ (A12) $\eta_{conc_c} = \frac{RT}{4F} \ln\left(\frac{p_{O_2}}{p_{O_{2TPB}}}\right)$ (A13)
A constant voltage offset was applied to account for gas crossover and internal current leakage, which are not explicitly captured in the electrochemical model	$\eta_{leakage} = DV$ (A14)

The fuel cell model described previously has been validated against experimental data obtained from a 25 cm^2 SolydEra anode-supported button cell [26] operating at 700 °C and ambient pressure, fed with 0.5 Nl/min of methane reformate containing H_2 (14.4%), H_2O (43.6%), CO (6.2%), CO_2 (24.7%), and CH_4 (11.1%) and 1.2 Nl/min of athomspheric air [26]. The cell features an anode-supported structure, with a Ni-YSZ anode (250 μm thick), a YSZ electrolyte (11 μm thick), and a cathode (49 μm thick). The cathode is characterized by a multilayer structure consisting of a 2 μm GDC barrier layer, a 19 μm LSCF-GDC electrode layer, and a 28 μm pure LSC current collector.

The experimental polarization and power curves were effectively matched (Figure A2), which demonstrates the model's ability to accurately reproduce the cell's electrochemical behavior.

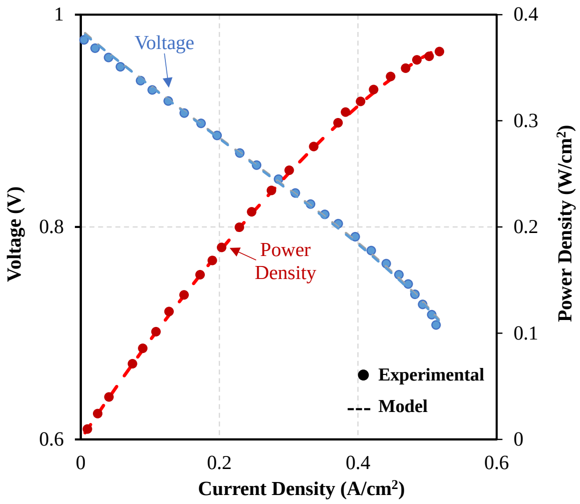

Figure A2. Experimental and numerical polarization (blue) and power (red) curves for the SolydEra anode-supported SOFC operating at 700 °C with methane reformate products (H_2 14.4%, H_2O 43.6%, CO 6.2%, CO_2 24.7%, CH_4 11.1%) and air.

For the purposes of this study, the same validated cell has been assumed to operate at 750 °C under direct ammonia feeding, and used as the elementary unit of the proposed SOFC-based propulsion system. This assumption is supported by experimental evidence demonstrating that SolydEra fed with direct ammonia have shown promising performance results [27]. Table A2 reports the operating conditions and of the modelled cell operating with ammonia

Table A2. Operating conditions of the proposed direct ammonia -fueled cell

Parameter	Unit	Value
Cell temperature	° C	750
Cell pressure	bar	1
Anode feed composition	%	100 NH_3
Cathode feed composition	-	Atmospheric air
Fuel utilization factor	-	0.8
Current density at rated power	A/cm^2	0.51
Voltage at rated power	V	0.81

Acknowledgment

This research has been supported by the Italian Government (LYRICA, PRIN project 2022, code 2022M7BHN7).

References

[1] IEA, "International Shipping," Paris, 2022. [Online]. Available: https://www.iea.org/reports/international-shipping

[2] IMO, "Fourth IMO GHG Study 2020 Full Report," *International Maritime Organization*, vol. 6, no. 11, pp. 951–952, 2021.
[3] X. Wang, J. Zhu, and M. Han, "Industrial Development Status and Prospects of the Marine Fuel Cell: A Review," *Journal of Marine Science and Engineering*, vol. 11, no. 2, 2023, doi: 10.3390/jmse11020238.
[4] Bureau Veritas Marine&Offshore, "An overview of ammonia as fuel for ships." https://marine-offshore.bureauveritas.com/shipping-decarbonization/future-fuels/ammonia? (accessed May 16, 2025).
[5] P. A. Duong and H. Kang, "Ammonia as fuel for marine dual-fuel technology: A comprehensive review," *Fuel Processing Technology*, vol. 272, no. December 2024, p. 108205, 2025, doi: 10.1016/j.fuproc.2025.108205.
[6] L. N. Henderik, "Solid Oxide Fuel Cell Propulsion System Fueled by Ammonia," Delft University of Technology, 2020.
[7] S. Di Micco, M. Minutillo, L. Mastropasqua, V. Cigolotti, and J. Brouwer, "Ammonia-based Solid Oxide Fuel Cell for zero emission maritime power: a case study," *E3S Web of Conferences*, vol. 334, 2022, doi: 10.1051/e3sconf/202233406007.
[8] A. A. Koekkoek, "An ammonia-fuelled solid oxide fuel cell - internal combustion engine hybrid system for ships," Delft University of Technology, 2021.
[9] K. H. Kalstad, "Ammonia Fuelled Solid Oxide Fuel Cell to Power Maritime Applications," University of Adger, 2021.
[10] E. Visone, "Future Scenarios for Ro-Pax Concept Design," Università degli Studi di Napoli Federico II, Scuola Politecnica e delle Scienze di Base, 2017.
[11] Wärtsilä, "Wärtsilä 32 product guide," 2021.
[12] B. Turi, "SolydEra: High efficiency solutions," in *Italian Hydrogen Expo*.
[13] "Alma Clean Power successfully tests 100 kW direct ammonia fuel cell system," 2024. https://almacleanpower.com/news/alma-clean-power-successfully-tests-100-kw-direct-ammonia-fuel-cell-system (accessed May 29, 2025).
[14] J. Fan *et al.*, "Thermal management of solid oxide fuel cells with liquid metal," *International Journal of Hydrogen Energy*, vol. 48, no. 28, pp. 10659–10670, 2023, doi: 10.1016/j.ijhydene.2022.11.308.
[15] C. Li, K. Cheng, B. Li, H. Liu, J. Qin, and L. Wei, "Feasibility study on supercritical fuel cooled solid oxide fuel cell stack with internal reforming," *International Journal of Hydrogen Energy*, vol. 50, pp. 312–322, 2024, doi: 10.1016/j.ijhydene.2023.08.133.
[16] B. van Veldhuizen, S. Diethelm, D. Sahnen, A. Thomas, L. van Biert, and K. Visser, "Upscaling and Design of an SOFC System for Marine Applications," in *International Marine Conference*, 2023, no. November. [Online]. Available: https://www.researchgate.net/publication/375605556
[17] H. Fan, X. Xu, N. Abdussamie, P. S. L. Chen, and A. Harris, "Comparative study of LNG, liquid hydrogen, and liquid ammonia post-release evaporation and dispersion during bunkering," *International Journal of Hydrogen Energy*, vol. 65, no. January, pp. 526–539, 2024, doi: 10.1016/j.ijhydene.2024.04.039.
[18] P.-W. Li, L. Schaefer, and M. K. Chyu, *Multiple transport processes in solid oxide fuel cells*, vol. 10. 2005. doi: 10.2495/1-85312-840-6/01.
[19] T. Hosoi, T. Yonekura, K. Sunada, and K. Sasaki, "Exchange Current Density of SOFC Electrodes: Theoretical Relations and Partial Pressure Dependencies Rate-Determined by Electrochemical Reactions," *Journal of The Electrochemical Society*, vol. 162, no. 1, pp. F136–F152, 2015, doi: 10.1149/2.0561501jes.
[20] P. Costamagna, A. Selimovic, M. Del Borghi, and G. Agnew, "Electrochemical model of the integrated planar solid oxide fuel cell (IP-SOFC)," *Chemical Engineering Journal*, vol. 102, no. 1, pp. 61–69, 2004, doi: 10.1016/j.cej.2004.02.005.

[21] D. Tapiero, D. Diskin, N. Tzabar, and L. Tartakovsky, “Performance of solid-oxide fuel cells fed with pure hydrogen and methanol steam reforming products – experimental study,” *International Journal of Hydrogen Energy*, vol. 50, pp. 1427–1440, 2023, doi: 10.1016/j.ijhydene.2023.07.180.
[22] K. Tseronis, I. K. Kookos, and C. Theodoropoulos, “Modelling mass transport in solid oxide fuel cell anodes: a case for a multidimensional dusty gas-based model,” *Chemical Engineering Science*, vol. 63, no. 23, pp. 5626–5638, 2008, doi: 10.1016/j.ces.2008.07.037.
[23] A. T. O. Dal’Toé, N. Padoin, K. Ropelato, and C. Soares, “Study of Correlations for the Prediction of the Diffusion Coefficients in Multicomponent Mixture,” in *XX Congresso Brasileiro de Engenharia Quìmica*, 2014, no. October 2014, pp. 6321–6328. doi: 10.5151/chemeng-cobeq2014-1853-17207-142352.
[24] V. Novaresio, M. Garcìa-Camprubì, S. Izquiredo, P. Asinari, and N. Fueyo, “Numerical Modeling of Mass-Transport in Solid-Oxide Fuel,” *Computer Physics Communications*, pp. 1–66, 2011.
[25] S. A. Hajimolana, M. A. Hussain, W. M. A. W. Daud, M. Soroush, and A. Shamiri, “Mathematical modeling of solid oxide fuel cells: A review,” *Renewable and Sustainable Energy Reviews*, vol. 15, no. 4, pp. 1893–1917, 2011, doi: 10.1016/j.rser.2010.12.011.
[26] M. Pagliari, D. Montinaro, E. Martelli, S. Campanari, and A. Donazzi, “Durability and kinetic effects of CO2-rich oxidizing streams on LSCF-based solid oxide fuel cells,” *Journal of Power Sources*, vol. 613, no. May, p. 234895, 2024, doi: 10.1016/j.jpowsour.2024.234895.
[27] N. Coppola *et al.*, “Comparison of the Electrochemical Performances of Solid Oxide Fuel Cells with Sputtered Thin Barrier Layers Fueled by Hydrogen or Ammonia,” *Crystals*, vol. 13, no. 7, 2023, doi: 10.3390/cryst13071040.